Real-time event-based formation control of a group of VTOL-UAVs

Jose Fermi Guerrero Castellanos, A. Vega-Alonzo, Nicolas Marchand, Sylvain Durand, J. Linares-Flores, G. Mino-Aguilar

Real-time event-based formation control of a group of VTOL-UAVs

J.F. Guerrero-Castellanos*, A. Vega-Alonzo*, N. Marchand†, S. Durand‡, J. Linares-Flores * and G. Mino-Aguilar*
*Autonomous University of Puebla (BUAP), Faculty of Electronics, Puebla, Mexico
Email: fermi.guerrero@correo.buap.mx
†GIPSA-lab laboratory, Control Systems Dept., SySCo team
CNRS-Univ. of Grenoble, ENSE3 BP 46, 38402 St Martin d'Hères Cedex, France,
Email: nicolas.marchand@gipsa-lab.inpg.fr
‡INSA Strasbourg and ICube, Strasbourg, France
Email: sylvain@durandchamontin.fr

***Abstract*—This paper presents the development of a collaborative event-based control applied to the problem of formation of a group of VTOL-UAVs (Vertical Take-off and Landing, Unmanned Aerial Vehicles) . Each VTOL-UAV decides, based on the difference of its current state (linear position and velocity) and its latest broadcast state, when it has to send a new value to its neighbors. The asymptotic convergence to average consensus or desired formation is depicted via a real-time implementation.**

I. Introduction

Motivated by applications in physics, biology and engineering the study of consensus of collections of agents (or dynamic systems) has become an important topic in control theory. Roughly speaking, consensus means to reach an agreement regarding a certain quantity of interest that depends on the state of all agents. A consensus algorithm (or protocol) is an interaction rule that specifies the information exchange between an agent and all of its neighbors on the network. Consensus problems have a long history in computer science and form the foundation of the field of distributed computing [1]. Distributed computation over networks has a tradition in systems and control theory *e.g.* [2] and [3].
Cooperative distributed control strategies for multiple vehicles have gained increased attention in recent years in the control community, owing to the fact that such strategies provide attractive solutions to large-scale multi-agent problems, both in terms of complexity in the formulation of the problem, as well as in terms of the computational load required for its solution. As an important branch of cooperative control, distributed cooperative attitude control for multiple rigid bodies has received much research attention. The motivation to consider rigid body dynamics comes from the fact that rigid body describes a very large class of physical systems of practical interest, *e.g.* spacecraft, UAVs, robot manipulators and wearable robots [4], [5].

An important aspect in the implementation of distributed algorithms is the communication and controller actuation schemes. With the development of embedded, miniaturized and interconnected systems, there is a growing interest in Networked Control Systems (NCSs) where the control loop is closed over a communication link [6], [7]. A network has several advantages, like flexibility in the configuration of the communication structure and the number of interconnected systems. However, it also has a considerable impact on the performance, notably because of communication delays and packet losses which avoid real-time control constraints to be meet and can even cause the instability of the control loop.

Recently, published works addressed resource aware implementations of the control law using event-based sampling, where the control law is event-driven. Such a paradigm calls for resources whenever they are indeed necessary, that is for instance when the dynamics of the controlled system varies, *i.e.* when some events occur. The development of event-based control strategies have their origins in the seminal works [8] and [9] where the the first event driven PID was developed. Event-based control usually relies on a triggering algorithm which takes the form of an event function $e : \mathcal{X} \to \mathbb{R}$ that indicates if one needs ($e \leq 0$) or not ($e > 0$) to update the control value. $\mathcal{X}$ in general represents the state space. The basic event-based control strategies consist in level-crossing approaches like in [10] where $\mathcal{X}$ represents the output system. Other level-crossing approaches were reported in [11][12]. In more sophisticate approaches, the function e takes the current state x as input and a memory m of x last time e became negative as in [13], [14]. Recent advances in event-triggered control can be classified into two main categories, Periodic Event-triggered Control scheme (PETC) and Continuous Event-triggered Control scheme (CETC). For PETC, a periodic sampling is given and the event function indicates the control must be updated at the next sampling instant [15] whereas in the Continuous Event-triggered Control scheme (CETC), the control function is updated instantaneously after the zeroing of the event function [16], [17], [18], [13].

In the context of cooperative distributed control, the event-based paradigm appears as a mean to reduce the communication bandwidth in the network since, contrary to the classical scheme, an event-based control invokes a communication between the different agents only when

This work has been partially supported by the LabEx PERSYVALLab (ANR-11-LABX-0025-01), by VIEP-BUAP under grant GUCJING17-I and by PRODEP-SEP in the framework of Integración de Redes Temáticas de Colaboración Académica.

a certain condition is satisfied. In [19] an event-based implementation of the consensus protocol is presented. In the aforementioned work all agents continuously monitor their neighbors states, then each agent updates its control law not only at its own event-times, but also whenever one of its neighbors triggers an event. Later in [20] these disadvantages are addressed, and the authors developed an event-based control strategy for multi-agent average consensus where measurement broadcasts are scheduled in an event-based fashion, such that continuous monitoring of the neighbors states is no longer required.

Although the aforementioned approaches have shown benefits, these works were developed in a continuous event-triggered context, which means that the event-triggered condition has to be monitored continuously and it is necessary to guarantee non zero inter-execution time (Zeno behavior).

The control strategy proposed in the present paper is more in the spirit of the one proposed in [20]. The proposed control technique is applied to the problem of consensus and formation of a group of VTOL-UAVs. Hence, each VTOL-UAV decides, based on the difference of its current state (linear position and velocity) and its latest broadcast state, when it has to send a new value to its neighbors. The asymptotic convergence to average consensus is guaranteed under such an event-triggered strategy. Numerical simulation are performed for the consensus of four quadrotors, where the effectiveness is illustrated via the comparison to traditional time-scheduled control. Besides the development of a collaborative event-triggered control, the hoped-for contribution of this paper is that of unification, so that the reader can see how mixing topics such as Unmanned Aerial Vehicles, nonlinear attitude control, and event-triggered collaborative control.

The paper is structured as follows. Section II contains mathematical preliminaires. In section III, the attitude control is given and an event-based strategy for position and velocity consensus is presented. Section IV is devoted to real-time implementation results, which show the effectiveness of the proposed algorithm. Finally, in section V some conclusions are presented.

II. Preliminaries

A. Graph theory

Consider $\mathcal{G} = \{\mathcal{V}, \mathcal{E}\}$ consisting of a set of vertices (or nodes) $\mathcal{V} = 1, ..., N$ and edges $\mathcal{E}$. If there is an edge (i, j) between nodes i and j, then i and j are called adjacent, i.e. $\mathcal{E} = (i, j) \in \mathcal{V} \times \mathcal{V} : i, j \ adjacent$. $\mathcal{G}$ is called undirected if $(i, j) \in \mathcal{E} \Leftrightarrow (i, j) \in \mathcal{E}$. The adjacency matrix A is defined by $a_{ij} = 1$ if i and j are adjacent and $a_{ij} = 0$ otherwise. A path from i to j is a sequence of distinct nodes, starting from i and ending with j, such that each pair of consecutive nodes is adjacent. If there is a path from i to j, then i and j are called connected. if all pairs of nodes in $\mathcal{G}$ are connected, then $\mathcal{G}$ is called connected. The distance $d(i, j)$ between two nodes is the number of edges of the shortest path from i to j. The diameter d of $\mathcal{G}$ is the maximum distance $d(i, j)$ over all pairs of nodes. The degree matrix D of $\mathcal{G}$ is the diagonal matrix with elements d_i equal to the cardinality of node i's neighbor set $N_i = \{j \in \mathcal{V} : (i, j) \in \mathcal{E}$. The Laplacian matrix $\mathcal{L}$ of $\mathcal{G}$ is defined as $\mathcal{L} = D - A$. For undirected graphs, $\mathcal{L}$ is symmetric and positive semi-definite, i.e., $\mathcal{L} = \mathcal{L}^T \geq 0$. The row sums of $\mathcal{L}$ are zero. Thus, the vector of ones $\mathbb{1}$ is an eigenvector corresponding to eigenvalue $\lambda_i(\mathcal{G}) = 0$, i.e., $\mathcal{L}\mathbb{1} = 0$. For connected graphs, $\mathcal{L}$ has exactly one zero eigenvalue, and the eigenvalues can be listed in increasing order $0 = \lambda_1(\mathcal{G}) < \lambda_2(\mathcal{G}) \leq ... \leq \lambda_N(\mathcal{G})$. The second eigenvalue $\lambda_2(\mathcal{G})$ is call the algebraic connectivity.

B. VTOL-UAVs model

Firstly, assume that a VTOL-UAV can be modeled as a rigid body (see Fig. 1). Then, consider two orthogonal right-handed coordinate frames: the body coordinate frame, $\mathbf{E}^b = [\vec{e}_1{}^b, \vec{e}_2{}^b, \vec{e}_3{}^b]$, located at the center of mass of the rigid body and the inertial coordinate frame, $\mathbf{E}^f = [\vec{e}_1{}^f, \vec{e}_2{}^f, \vec{e}_3{}^f]$, located at some point in the space. The rotation of the body frame $\mathbf{E}^b$ with respect to the fixed frame $\mathbf{E}^f$ is represented by the attitude matrix $R \in SO(3) = \{R \in \mathbb{R}^{3\times3} : R^T R = I, \det R = 1\}$.

The cross product between two vectors $\xi, \chi \in \mathbb{R}^3$ is

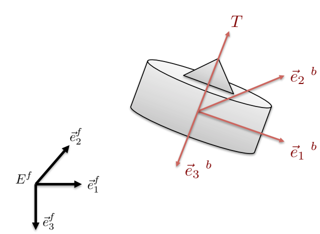

Fig. 1. Body-fixed and inertial reference frame

represented by a matrix multiplication $[\xi^\times]\chi = \xi \times \chi$, where $[\xi^\times]$ is the well known skew-symmetric matrix.

The n-dimensional unit sphere embedded in $\mathbb{R}^{n+1}$ is denoted as $\mathbb{S}^n = \{x \in \mathbb{R}^{n+1} : x^T x = 1\}$. Members of $SO(3)$ are often parametrized in terms of a rotation $\beta \in \mathbb{R}$ about a fixed axis $e_v \in \mathbb{S}^2$ by the map $\mathcal{U} : \mathbb{R} \times \mathbb{S}^2 \to SO(3)$ defined as

$$\mathcal{U}(\beta, e_v) := I_3 + \sin(\beta)[e_v^\times] + (1 - \cos(\beta))[e_v^\times]^2 \quad (1)$$

Hence, a unit quaternion, $q \in \mathbb{S}^3$, is defined as

$$q := \begin{pmatrix} \cos\frac{\beta}{2} \\ e_v \sin\frac{\beta}{2} \end{pmatrix} = \begin{pmatrix} q_0 \\ q_v \end{pmatrix} \in \mathbb{S}^3 \quad (2)$$

$q_v = (q_1 \ \ q_2 \ \ q_3)^T \in \mathbb{R}^3$ and $q_0 \in \mathbb{R}$ are known as the vector and scalar parts of the quaternion respectively. q represents an element of $SO(3)$ through the map $\mathcal{R} : \mathbb{S}^3 \to SO(3)$ defined as

$$\mathcal{R} := I_3 + 2q_0[q_v^\times] + 2[q_v^\times]^2 \quad (3)$$

Note that $R = \mathcal{R}(q) = \mathcal{R}(-q)$ for each $q \in \mathbb{S}^3$, *i.e.* quaternions q and $-q$ represent the same physical attitude.

Denoting by $\omega = (\omega_1 \ \ \omega_2 \ \ \omega_3)^T$ the angular velocity vector of the body coordinate frame, $\mathbf{E}^b$ relative to the inertial coordinate frame, $\mathbf{E}^f$, expressed in $\mathbf{E}^b$, the kinematics equation is given by

$$\begin{pmatrix} \dot{q}_0 \\ \dot{q}_v \end{pmatrix} = \frac{1}{2}\begin{pmatrix} -q_v^T \\ I_3 q_0 + [q_v^\times] \end{pmatrix}\omega = \frac{1}{2}\Xi(q)\omega \quad (4)$$

The attitude error is used to quantify the mismatch between two attitudes. If q defines the current attitude quaternion and q_d is the desired quaternion, *i.e.* the desired orientation, then the quaternion that represents the attitude error between the current orientation and the desired one is given by

$$\tilde{q} = q_d^{-1} \otimes q = (\tilde{q}_0 \ \tilde{q}_v{}^T)^T \quad (5)$$

where q^{-1} is the complementary rotation of the quaternion q which is given by $q^{-1} = (q_0 \quad -q_v^T)^T$ and $\otimes$ denotes the quaternion multiplication [21]. In the case that the current quaternion and the desired one coincide, the quaternion error becomes $\tilde{q} = (\pm 1 \; 0^T)^T$.
As it was mentioned before, the quaternion representation is redundant. As a consequence, the error mathematical model has two equilibrium and this fact must be considered in the stability analysis [22].
Now, consider a group of N-VTOL UAVs modeled as rigid bodies (see Fig. 2). Then according to the aforementioned and to [23], the six degrees of freedom model (position and attitude) of the system can be separated into translational and rotational motions, represented respectively by Σ_{T_i} and Σ_{R_i} in equation (6) and (7).

$$\Sigma_{T_i} : \begin{cases} \dot{p}_i = v_i \\ \dot{v}_i = -g\vec{e}_3^{\,f} + \dfrac{1}{m_i} R_i^T T_i \vec{e}_{3_i}^{\,b} \end{cases} \tag{6}$$

$$\Sigma_{R_i} : \begin{cases} \dot{q}_i = \dfrac{1}{2}\Xi(q_i)\omega_i \\ J_i\dot{\omega}_i = -[\omega_i^\times] J\omega_i + \Gamma_i \end{cases} \tag{7}$$

with $i \in \mathcal{N} = \{1, ..., N\}$. m_i denotes the mass of the ith VTOL-UAV and J_i its inertial matrix expressed in $\mathbf{E}_i^b$. g is the gravity acceleration and $\vec{e}_{3_i}^{\,b} = \vec{e}_3^{\,f} = (0\ 0\ 1)^T$. $p_i \in \mathbb{R}^3$ represents the position of the aircraft's center of gravity, which coincides with the origin of frame $\mathbf{E}_i^b$, with respect to frame $\mathbf{E}^f$, $v_i \in \mathbb{R}^3$ its linear velocity in $\mathbf{E}^f$, and $\omega_i \in \mathbb{R}^3$ denotes the angular velocity expressed in $\mathbf{E}_i^b$. $\Gamma_i \in \mathbb{R}^3$ depends on the couples generated by the actuators, aerodynamic couples and external couples (environmental forces). In this paper, it is assumed that these torques are only generated by the actuators. $-T_i\vec{e}_{3_i}^{\,b}$ is the total thrust, expressed in $\mathbf{E}_i^b$.

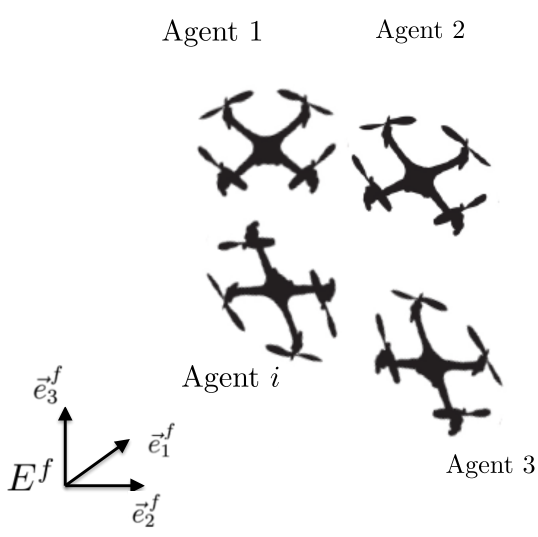

Fig. 2. Group of N-VTOL UAVs

III. Attitude and position control

In this subsection, a control law that stabilizes the system described by (6) and (7) is proposed.

Definition 3.1: Given a positive constant M, a continuous, nondecreasing function $\sigma_M : \mathbb{R} \to \mathbb{R}$ is defined by

$$\begin{array}{l} (1)\sigma_M(s) = s \text{ if } |s| < M; \\ (2)\sigma_M(s) = \text{sign}(s)M \text{ elsewhere;} \end{array} \tag{8}$$

Then, one has the following result reported previously in [23] for the attitude stabilization of rigid bodies.

Theorem 3.2: Consider the ith rigid body rotational dynamics described by (7) and the attitude error defined in (5) with the following bounded control inputs $\Gamma_i = (\Gamma_i^1\ \Gamma_i^2\ \Gamma_i^3)^T$ such that

$$\Gamma_i^l = -\sigma_{M_i^l}\left(\frac{\kappa_i \omega_i^l}{\rho_i^l} + \kappa_i \tilde{q}_{v_i}^{\;l}\right) \tag{9}$$

where $i \in \mathcal{N} = \{1, ..., N\}$. $\sigma_{M_i^l}(\cdot)$ with $l \in \{1, 2, 3\}$ are saturation functions as defined above. M_i^l represents the physical bound on the jth torque of the ith rigid body. κ_i is a real parameter such that $0 < \kappa_i \leq \min_l M_i^l/2$. ρ_i^l are strictly positive real parameters. Then the inputs (9) asymptotically stabilize the rigid body to the desired attitude q_{d_i} (*i.e.* $\tilde{q}_{0_i} = 1, \tilde{q}_{v_i} = 0, \omega_i = 0$) with a domain of attraction for the attitude error and angular velocity equal to $\mathbb{S}^3 \times \mathbb{R}^3 \setminus (-1\ 0^T\ 0^T)^T$.

Proof: The proof follows the one presented in [23]. ■

Now, the objective is to design a control law which stabilizes a group of VTOL-UAV to a certain position in the space (consensus problem), having the attitude stabilization problem solved. Consider (6) and (7). Note that the rotation matrix R_i can be parameterized in function of Euler angles, through the map $\mathcal{R}(\phi, \theta, \psi) : \mathbb{R}^3 \to SO(3)$

$$R = \mathcal{R}(\phi, \theta, \psi) = \\ \begin{pmatrix} \mathrm{C}\psi\ \mathrm{C}\theta & \mathrm{S}\psi\ \mathrm{C}\theta & -\mathrm{S}\theta \\ \mathrm{C}\psi\ \mathrm{S}\theta\ \mathrm{S}\phi - \mathrm{S}\psi\ \mathrm{C}\theta & \mathrm{S}\phi\ \mathrm{S}\theta\ \mathrm{S}\psi + \mathrm{C}\psi\ \mathrm{C}\phi & \mathrm{C}\theta\ \mathrm{S}\phi \\ \mathrm{C}\psi\ \mathrm{C}\phi\ \mathrm{S}\theta + \mathrm{S}\psi\ \mathrm{S}\phi & \mathrm{S}\theta\ \mathrm{S}\psi\ \mathrm{C}\phi - \mathrm{C}\psi\ \mathrm{S}\phi & \mathrm{C}\theta\ \mathrm{C}\phi \end{pmatrix}, \tag{10}$$

Assume that using the control law (9), one can stabilize the yaw dynamics of ith VTOL, that is $\psi_i = 0$. Then, after a sufficiently long time, system (6) becomes:

$$\begin{pmatrix} \dot{p}_{1_i} \\ \dot{p}_{2_i} \\ \dot{p}_{3_i} \end{pmatrix} = \begin{pmatrix} v_{1_i} \\ v_{2_i} \\ v_{3_i} \end{pmatrix}, \tag{11}$$

$$\begin{pmatrix} \dot{v}_{1_i} \\ \dot{v}_{2_i} \\ \dot{v}_{3_i} \end{pmatrix} = \begin{pmatrix} \frac{T_i}{m_i}\cos\phi_i \sin\theta_i \\ -\frac{T_i}{m_i}\sin\phi_i \\ \frac{T_i}{m_i}\cos\phi_i\cos\theta_i + g \end{pmatrix} \tag{12}$$

θ_i and ϕ_i can be viewed as an intermediate input to control (11)-(12). With an appropriate choice of these target configuration as proposed in [24], [25], it will be possible to transform (11)-(12) into three double integrators. For this, let us define

$$\begin{aligned} \theta_{d_i} &:= \arctan\left(\frac{r_{1_i}}{r_{3_i} + g}\right), \\ \phi_{d_i} &:= \arctan\left(\frac{-r_{2_i}}{\sqrt{r_{1_i}^2 + (r_{3_i} + g)^2}}\right) \end{aligned} \tag{13}$$

where r_{1_i}, r_{2_i} and r_{3_i} will be defined after. Then, choose as positive thrust the input control

$$T_i = m_i\sqrt{r_{1_i}^2 + r_{2_i}^2 + (r_{3_i} + g)^2} \tag{14}$$

By taking (13)-(14), it follows

$$\Sigma_{1_i} := \begin{cases} \dot{p}_{1_i} = v_{1_i} \\ \dot{v}_{1_i} = r_{1_i} \end{cases} \tag{15}$$

$$\Sigma_{2_i} := \begin{cases} \dot{p}_{2_i} = v_{2_i} \\ \dot{v}_{2_i} = r_{2_i} \end{cases} \tag{16}$$

$$\Sigma_{3_i} := \begin{cases} \dot{p}_{3_i} = v_{3_i} \\ \dot{v}_{3_i} = r_{3_i} \end{cases} \tag{17}$$

Now the aim is to adapt and apply a control law and a triggering rule, previously developed in [20], in order to determine, based on local information, when the ith VTOL-UAV (agent) has to trigger and broadcast a new state value to its neighbors, such that all agents' states converge to the average of their initial conditions. Each agent consists of a position controller as show in Fig. 3 In this case the position controller of system i monitors its own state $\xi_i = (p_i^T \ v_i^T)^T$ continuously, with $p_i = (p_{1_i} \ p_{2_i} \ p_{3_i})^T$ and $v_i = (v_{1_i} \ v_{2_i} \ v_{3_i})^T$. Based on local information, it decides when to broadcast its current state over the network. The latest broadcast state of system i given by $\hat{\xi}_i(t) = \xi_i(t_k^i) = (\hat{p}_i^T \ \hat{v}_i^T)^T$, $t \in [t_k^i, t_{k+1}^i[$, where $t_0^i, t_1^i, t_2^i...$ is the sequence of event times of agent i.

Hence a simple consensus algorithm to reach an agreement regarding the state of N VTOL-UAVs can be expressed:

$$r_{s_i} = -\sum_{j\in N_i}(\hat{p}_{s_i} - \hat{p}_{s_j}) - \mu\sum_{j\in N_i}(\hat{v}_{s_i} - \hat{v}_{s_j}) \tag{18}$$

with $s \in \{1, 2, 3\}$, $i \in \mathcal{N} = \{1, ..., N\}$ and $\mu \in \mathbb{R} > 0$. Let us define the following measurement errors for the linear position and velocity

$$\begin{aligned} e_{p_s,i}(t) &= \hat{p}_{s_i}(t) - p_{s_i}(t) \\ e_{v_s,i}(t) &= \hat{v}_{s_i}(t) - v_{s_i}(t) \\ e_{p,i}(t) &= (e_{p_1,i}^T \ e_{p_2,i}^T \ e_{p_3,i}^T)^T \\ e_{v,i}(t) &= (e_{v_1,i}^T \ e_{v_2,i}^T \ e_{v_3,i}^T)^T \end{aligned} \tag{19}$$

Furthermore, let us define the stack vectors $P_s(t) = (p_{s_1}(t)...p_{s_N}(t))^T$, $V_s(t) = (v_{s_1}(t)...v_{s_N}(t))^T$, and $\hat{P}_s(t) = (\hat{p}_{s_1}(t)...\hat{p}_{s_N}(t))^T$, $\hat{V}_s(t) = (\hat{v}_{s_1}(t)...\hat{v}_{s_N}(t))^T$, $E_{p_s} = (e_{p_s,1}(t)...e_{p_s,N}(t))^T$ and $E_{v_s} = (e_{v_s,i}(t)...e_{v_s,N}(t))^T$.

Hence, the control law (18) can be rewritten as

$$r_s = -\mathcal{L}(P_s(t) + \mu V_s(t) + E_{p_s}(t) + \mu E_{v_s}(t)) \tag{20}$$

Let $\bar{P}(t)$ and $\bar{V}(t)$ be $\bar{P}(t) = (P_1^T \ P_2^T \ P_3^T)^T$, $\bar{V} = (V_1^T \ V_2^T \ V_3^T)^T$ and $\bar{E}_p(t) = (E_{p_1}^T \ E_{p_2}^T \ E_{p_3}^T)^T$, $\bar{E}_v(t) = (E_{v_1}^T \ E_{v_2}^T \ E_{v_3}^T)^T$. Then, the closed-loop system becomes

$$\begin{pmatrix} \dot{\bar{P}} \\ \dot{\bar{V}} \end{pmatrix} = \Upsilon \begin{pmatrix} \bar{P} \\ \bar{V} \end{pmatrix} - \Upsilon_E \begin{pmatrix} \bar{E}_p(t) \\ \mu\bar{E}_v(t) \end{pmatrix} \tag{21}$$

where

$$\Upsilon = \begin{pmatrix} 0_{3N\times3N} & I_{3N\times3N} \\ -(I_{3N\times3N}\otimes\mathcal{L}) & -(I_{3N\times3N}\otimes\mu\mathcal{L}) \end{pmatrix} \tag{22}$$

and

$$\Upsilon_E = \begin{pmatrix} 0_{3N\times3N} & 0_{3N\times3N} \\ (I_{3N\times3N}\otimes\mathcal{L}) & (I_{3N\times3N}\otimes\mathcal{L}) \end{pmatrix} \tag{23}$$

where the term $\otimes$ denotes the Kronecker product.
Define the average velocity b_s and the average position $a_s + b_s t$ of all the agents, with

$$\begin{aligned} a_s &= \frac{1}{N}\sum_{i\in\mathcal{V}} p_{s_i}(0) \\ b_s &= \frac{1}{N}\sum_{i\in\mathcal{V}} v_{s_i}(0) \end{aligned} \tag{24}$$

Then, one has the following result:

Corollary 3.3: Consider the group of VTOL-UAVs (11)-(12) with control laws (13)-(14) and (18). Suppose the trigger function is given by

$$\begin{aligned} f_i(t, e_{p,i}(t), e_{v,i}(t)) = &\| (e_{p,i}^T(t) \ \mu e_{v,i}^T(t))^T \| \\ &- (c_0 + c_1 e^{-\alpha t}) \end{aligned} \tag{25}$$

with constants $c_0, c_1 \geqslant 0$ and $c_0 + c_1 > 0$, and $0 < \alpha < | \ \mathrm{Re}(\lambda_3(\Upsilon)) \ |$. Then, for all initial conditions $\xi_i(0) = (p_i^T(0) \ v_i^T(0))^T$ the average velocity and average position consensus are reached, with an error that depends on the value of c_0 of the trigger function, the eigenvalues of Υ and the number of agents in the graph [20].

A. Formation control

Let Δ be a set of relative, desired inter-agent distances, that is,

$$\Delta = \{\delta_{ij} \in \mathbb{R} \mid \delta_{ij} > 0, i, j = 1, ..., N, i \neq 0\} \tag{26}$$

with $\delta_{ij} = \delta_{ji}$ and where it is assumed that Δ is a feasible formation, that is, there are points $\zeta_1, .., \zeta_n \in \mathbb{R}^3$ such that

$$\|\zeta_i - \zeta_j\| = \delta_{ij} \tag{27}$$

Since consensus algorithms can be extended to formation control if the formation is represented by vectors of relative positions of neighboring agents, the control law (18) can be used for this objective. In this case one has:

$$r_{s_i} = \sum_{j\in N_i}(\hat{p}_{s_i} - \hat{p}_{s_j} - \delta_{s_{ij}}) - \mu\sum_{j\in N_i}(\hat{v}_{s_i} - \hat{v}_{s_j}) \tag{28}$$

with $s \in \{1, 2, 3\}$, $i \in \mathcal{N} = \{1, ..., N\}$ and $\mu \in \mathbb{R} > 0$.

The Fig.3 depicts the control law running in the ith vehicle.

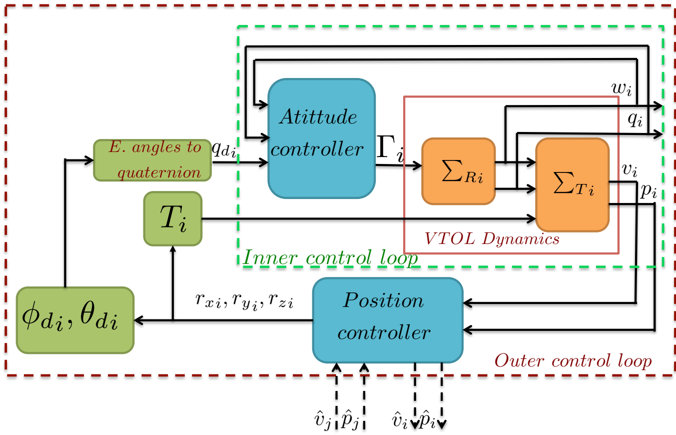

Fig. 3. Block diagram of the even-based control strategy

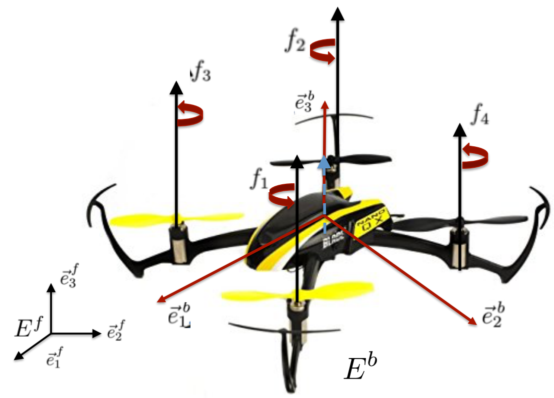

Fig. 4. Quadrotor: fixed frame $\mathbf{E}^f = [\vec{e}_1^{\,f}, \vec{e}_2^{\,f}, \vec{e}_3^{\,f}]$ and body-fixed frame $\mathbf{E}^b = [\vec{e}_1^{\,b}, \vec{e}_2^{\,b}, \vec{e}_3^{\,b}]$

IV. Experimental results

In this section, the proposed control algorithms are verified and illustrated through a real-time implementation. The VTOL vehicle considered is the well known four-rotor mini-helicopter so called quadrotor, which is modeled as (6)-(7). Several experiments were carried out with a focus on the formation.

A. Four-rotor mini-helicopter model

The quadrotor is a small aerial vehicle that belongs to the VTOL (Vertical Taking Off and Landing) class of aircrafts. It is lifted and propelled, forward and laterally, by controlling the rotational speed of four blades mounted at the four ends of a simple cross and driven by four DC Brushless motors (BLDC). On such a platform (see Fig. 4), given that the front and rear motors rotate counter-clockwise while the other two rotate clockwise, gyroscopic effects and aerodynamic torques tend to cancel each other out in trimmed flight. The rotation of the four rotors generates a vertical force, called the thrust T, equal to the sum of the thrusts of each rotor ($T = f_1 + f_2 + f_3 + f_4$). The pitch movement θ is obtained by increasing/decreasing the speed of the rear motor while decreasing/increasing the speed of the front motor. The roll movement ϕ is obtained similarly using the lateral motors. The yaw movement ψ is obtained by increasing/decreasing the speed of the front and rear motors while decreasing/increasing the speed of the lateral motors. In order to avoid any linear movement of the quadrotor, these maneuvers should be achieved while maintaining a value of the total thrust T that balances the aircraft weight. In order to model the system's dynamics, two frames are defined: a fixed frame in the space $\mathbf{E}^f = [\vec{e}_1{}^f, \vec{e}_2{}^f, \vec{e}_3{}^f]$ and a body-fixed frame $\mathbf{E}^b = [\vec{e}_1{}^b, \vec{e}_2{}^b, \vec{e}_3{}^b]$, attached to the quadrotor at its center of gravity, as shown in Fig. 4.

The components of the control torque vector Γ generated by the rotors are given by:

$$\begin{aligned} \Gamma^1 &= d b_m (u_{m3} - u_{m4}) \\ \Gamma^2 &= d b_m (u_{m1} - u_{m2}) \\ \Gamma^3 &= k_m(-u_{m1} + u_{m2} - u_{m3} + u_{m4}) \\ T &= b_m \sum_{\bar{l}=1}^{4} u_{m\bar{l}} \end{aligned} \tag{29}$$

with d being the distance from one rotor to the center of mass of the quadrotor. Since the motors are divers by Pulse Width Modulated (PWM) control signal, the signals $u_{m_{(1,2,3,4)}}$ are expressed in seconds, that is, the time during which the PWM control signal is in high state. In experimentation the Nano QX is used, and a "X" configuration is adopted, then the control torque becomes, $\bar{\Gamma}_1 = \frac{1}{\sqrt{2}}(\Gamma^1 - \Gamma^2)$, $\bar{\Gamma}_2 = \frac{1}{\sqrt{2}}(\Gamma^1 + \Gamma^2)$ and $\bar{\Gamma}_3 = \Gamma_3$

B. Experimental set-up

In order to test the effectiveness of the proposed control law, a set of experiments were performed. The aerial system consists on the machanical structure of Nano QX four-rotor, which on-board computer system was modified in order to implement the control laws . The attitude control for the quadrotor is embedded in a Microwii Copter board, which has rate gyros, accelerometers for attitude estimation and the ATMega32u4 as processor. Then, a ground station obtains the position and estimates the velocity of the quadrotor using the Vicon Tracker system and T40s cameras (add references). With this system it is possible to compute the linear position and estimate the linear velocity up to 100Hz. The estimated states are sent to MATLAB/Simulink through a UDP frame every 2ms. The position control algorithm is implemented in real-time at 200Hz on a computer using xPC target toolbox. The control variables are finally sent back to the quadrotor on the Microwii, through a GIPSA-lab's built-in bridge that converts UDP frames to Bluetooth or DSM2 protocol. An overview of the MOCA flying Arena [26] and the total hardware architecture [27] is presented in Fig. 5 and 6, respectively.

A set of experiments were performed in order to evaluate the performance of the proposed consensus and formation control. Here a scenario is shown. The parameters of the control law (9) are selected according to the characteristics of the actuators and those of the hexacopter presented previously. These control gains are: $\rho_{1,2} = 4.2$, $\rho_3 = 1.74$ and $\kappa = 0.075$. For this propose, three agents are employed, each one represents a VTOL - UAV in real-time. The communication graph implemented in the collaborative system is illustrated in Fig. 7. The real-time implementation was performed in a

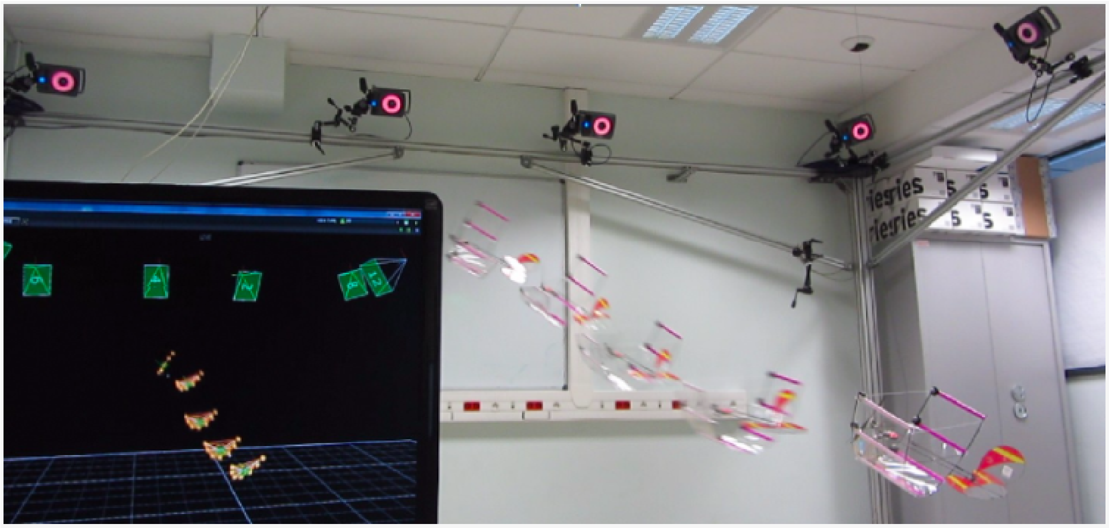

Fig. 5. The MOCA flying Arena equipped with 12 motion-capture cameras (VICON T-40s) and its flying space is about 5.6x6.6x2.9 m^3

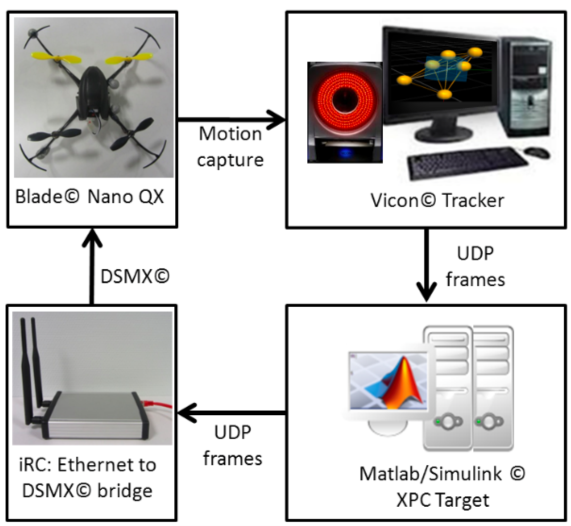

Fig. 6. Quadrotor control system process at MOCA flying Arena

time stamp of 70 seconds. For the event function, $c_0 = 0.02$ and for simplicity $c_1 = 0$ was chosen. The sampling time is 0.01 seconds. In this experiment, the control objective is to guarantee that the three vehicles maintain a pre-defined formation shape, described by an equilateral triangle. The desired inter-vehicle relative position vector are shown in Table I and the initial conditions of each vehicle are shown in Table II with angular and linear velocity equal to zero. The obtained results in this case are given in Fig. 8 where the first shape in formation routine is attained and Figs. 9 and 10, which depict the attitude and positions vectors in space for each agent, respectively. Here the Euler angles are depicted since they are more intuitive, however the attitude control law uses quaternions. One observers from these figures that the control objective is achieved using the event-triggered strategy control.

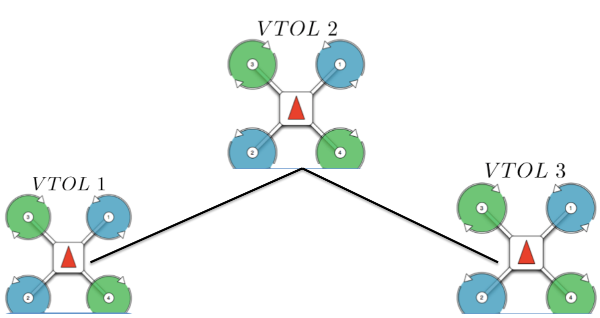

Fig. 7. Comunication between agents represented by the connected and undirected graph $\mathcal{G}$

The events occurrences are shown in Fig. 11, which illustrates that during the first seconds there exist several occurrences and they are reduced while the vehicle reaches the formation. Remember that an event takes place when the i agent broadcasts its position and velocity to the neighbors. In the classical frame (time-triggered control), the state should be broadcast 7000 times for a span of 70 seconds, since the sampling time is 0.01 sec. With the proposed approach, the number of events per agent was 5602 (VTOL 1), 5159 (VTOL 2), 5298 (VTOL 3), which represents (in average) a reduction of 25%. A video of the experimental results is shown in https://drive.google.com/open?id=0B2AkQ78IxANtS29nLXFUSjZsTGM.

V. Conclusion

In this work, a collaborative control strategy applied the problem of formation of a group of VTOL is proposed. The attitude control and formation were tested real real-time. Although the operation of the designed strategies is an important point of this work, we strongly believe that the greatest contribution is the development of an event-based control strategy used in the transmission of states between agents. This event-based control algorithm reduces the number of transmissions between agents approximately by 25 %, which demonstrate the superiority in terms of load on the communication medium.

Future work will address the real-time experimentation in an outdoor scenario.

Formation shape		
Agent	$\zeta(t_1)$	$\zeta(t_2)$
VTOL 1	(0.5, 0, 1)	(0, 0.5, 1)
VTOL 2	(-0.5, 0, 1)	(0, -0.5, 1)
VTOL 3	(0, -0.5, 1)	(0.5, 0, 1)

TABLE I. TWO FORMATIONS SPECIFIED THROUGH DESIRED INTER-AGENT DISTANCES.

Inital conditions		
Agent	Attitude (ϕ, θ, ψ) ($^\circ$)	Position (x, y, z) (m)
VTOL 1	(-18, 13, 5)	(0.7, 0.4, 0.13)
VTOL 2	(-3, -10, 30)	(0.1, 0.2, 0.13)
VTOL 3	(8, 10, -20)	(-0.7, -0.4, 0.13)

TABLE II. INITAL CONDITIONS

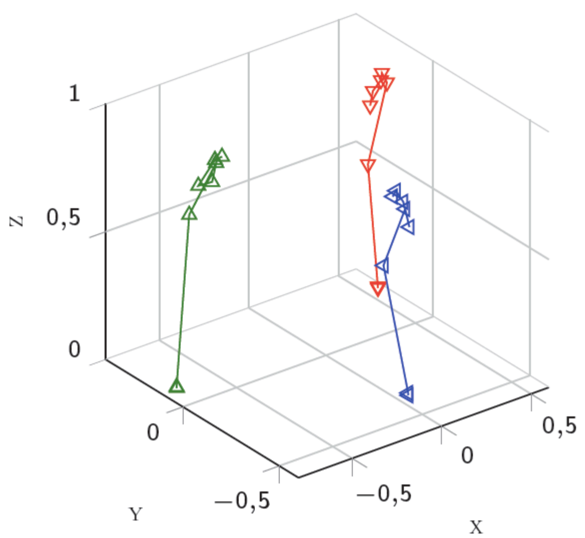

Fig. 8. First shape in formation routine

REFERENCES

[1] N. A. Lynch, *Distributed algorithms*. Morgan Kaufmann, 1996.

[2] V. Borkar and P. P. Varaiya, "Asymptotic agreement in distributed estimation," *Automatic Control, IEEE Transactions on*, vol. 27, no. 3, pp. 650–655, 1982.

[3] J. N. Tsitsiklis, "Problems in decentralized decision making and computation." DTIC Document, Tech. Rep., 1984.

[4] A. Abdessameud and A. Tayebi, "Attitude synchronization of a group of spacecraft without velocity measurements," *Automatic Control, IEEE Transactions on*, vol. 54, no. 11, pp. 2642–2648, 2009.

[5] W. Ren, "Formation keeping and attitude alignment for multiple spacecraft through local interactions," *Journal of Guidance, Control, and Dynamics*, vol. 30, no. 2, pp. 633–638, 2007.

[6] R. Olfati-Saber and J. S. Shamma, "Consensus filters for sensor networks and distributed sensor fusion," in *Decision and Control, 2005 and 2005 European Control Conference. CDC-ECC'05. 44th IEEE Conference on*. IEEE, 2005, pp. 6698–6703.

[7] G. S. Seyboth, D. V. Dimarogonas, and K. H. Johansson, "Control of multi-agent systems via event-based communication," in *Proceedings of the 18th IFAC World Congress, 2011*, 2011.

[8] K. J. Åström and B. Bernhardsson, "Comparison of riemann and lebesque sampling for first order stochastic systems," in *Proceedings of the 41st IEEE Conference on Decision and Control, 2002*, vol. 2. IEEE, 2002, pp. 2011–2016.

[9] K.-E. Årzén, "A simple event-based PID controller," in *Preprints 14th World Congress of IFAC*, Beijing, P.R. China, Jan. 1999.

[10] S. Durand and N. Marchand, "An event-based pid controller with low computational cost," in *8th International Conference on Sampling Theory and Applications (SampTA'09)*, 2009, pp. Special–session.

[11] M. Velasco, P. Martí, and E. Bini, "On lyapunov sampling for event-driven controllers," in *Decision and Control, 2009 held jointly with the 2009 28th Chinese Control Conference. CDC/CCC 2009. Proceedings of the 48th IEEE Conference on*. IEEE, 2009, pp. 6238–6243.

[12] S. Durand, N. Marchand, and J. F. Guerrero Castellanos, "Simple Lyapunov Sampling for Event-Driven Control," in *18th IFAC World Congress (IFAC WC 2011)*, Milan, Italy, Aug. 2011, p. 7 p.

[13] N. Marchand, S. Durand, and J. F. Guerrero-Castellanos, "A general formula for event-based stabilization of nonlinear systems," *Automatic Control, IEEE Transactions on*, vol. 58, no. 5, pp. 1332–1337, 2013.

[14] J. Guerrero-Castellanos, J. Téllez-Guzmán, S. Durand, N. Marchand, J. Alvarez-Muñoz, and V. R. Gonzalez-Diaz, "Attitude stabilization of a quadrotor by means of event-triggered nonlinear control," *Journal of Intelligent & Robotic Systems*, vol. 73, no. 1-4, pp. 123–135, 2014.

[15] W. P. M. H. Heemels, M. C. F. Donkers, and A. R. Teel, "Periodic event-triggered control for linear systems," *IEEE Transactions on Automatic Control*, vol. 58, no. 4, pp. 847–861, 2013.

[16] P. Tabuada, "Event-triggered real-time scheduling of stabilizing control tasks," *Automatic Control, IEEE Transactions on*, vol. 52, no. 9, pp. 1680–1685, 2007.

[17] A. Anta and P. Tabuada, "To sample or not to sample: Self-triggered control for nonlinear systems," *Automatic Control, IEEE Transactions on*, vol. 55, no. 9, pp. 2030–2042, 2010.

[18] M. Mazo Jr, A. Anta, and P. Tabuada, "On self-triggered control for linear systems: Guarantees and complexity," in *Control Conference (ECC), 2009 European*. IEEE, 2009, pp. 3767–3772.

[19] D. V. Dimarogonas, E. Frazzoli, and K. H. Johansson, "Distributed event-triggered control for multi-agent systems," *IEEE Transactions on Automatic Control*, vol. 57, no. 5, pp. 1291–1297, 2012.

[20] G. S. Seyboth, D. V. Dimarogonas, and K. H. Johansson, "Event-based broadcasting for multi-agent average consensus," *Automatica*, vol. 49, no. 1, pp. 245–252, 2013.

[21] M. D. Shuster, "A survey of attitude representations," *Navigation*, vol. 8, no. 9, pp. 439–517, 1993.

[22] R. Schlanbusch, A. Loria, and P. J. Nicklasson, "On the stability and stabilization of quaternion equilibria of rigid bodies," *Automatica*, vol. 48, no. 12, pp. 3135–3141, 2012.

[23] J. F. Guerrero-Castellanos, N. Marchand, A. Hably, S. Lesecq, and J. Delamare, "Bounded attitude control of rigid bodies: Real-time experimentation to a quadrotor mini-helicopter," *Control Engineering Practice*, vol. 19, no. 8, pp. 790–797, 2011.

[24] R. Sepulchre, M. Jankovic, and P. V. Kokotović, *Constructive Nonlinear Control*. London: Springler, 1997.

[25] A. Zavala, I. Fantoni, and R. Lozano, "Global stabilization of a pvtol aircraft model with bounded inputs," *International Journal of Control*, vol. 76, no. 18, pp. 1833–1844, 2003.

[26] "Flying arena," http://www.gipsa-lab.fr/projet/RT-MaG/Equipment.php, March 2017.

[27] "Gipsa-lab equipment," http://www.gipsa-lab.grenoble-inp.fr, March 2017.

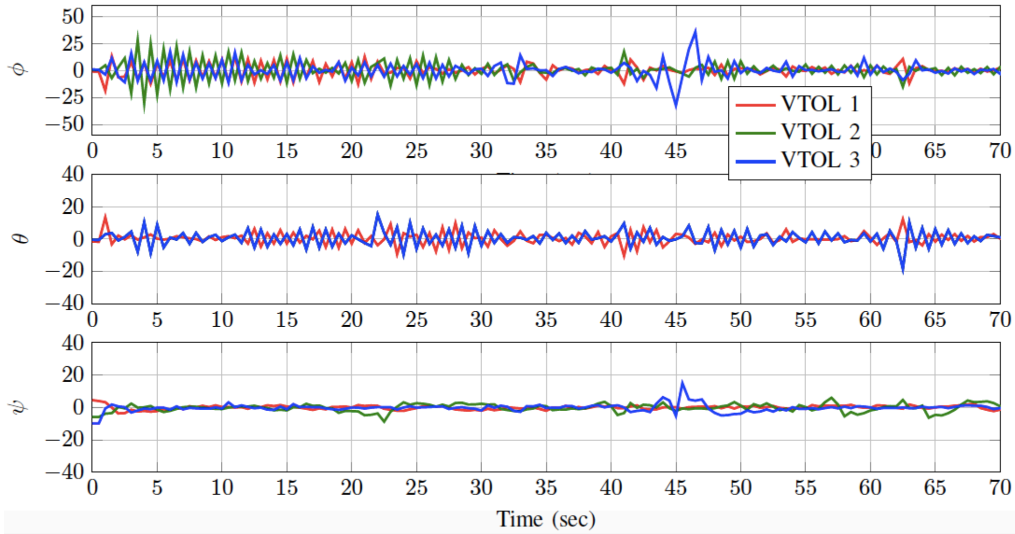

Fig. 9. Quadrotors' attitude

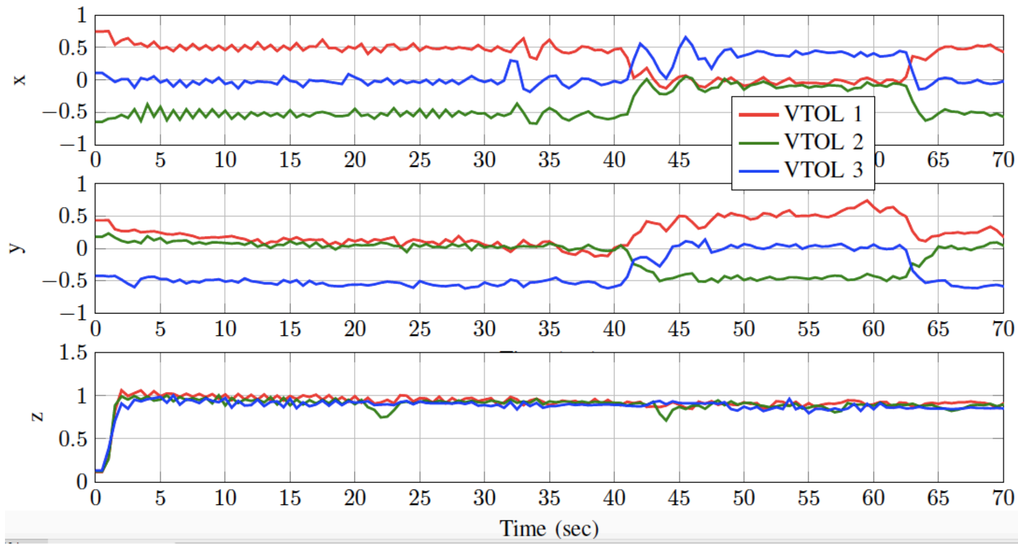

Fig. 10. Quadrotors' position

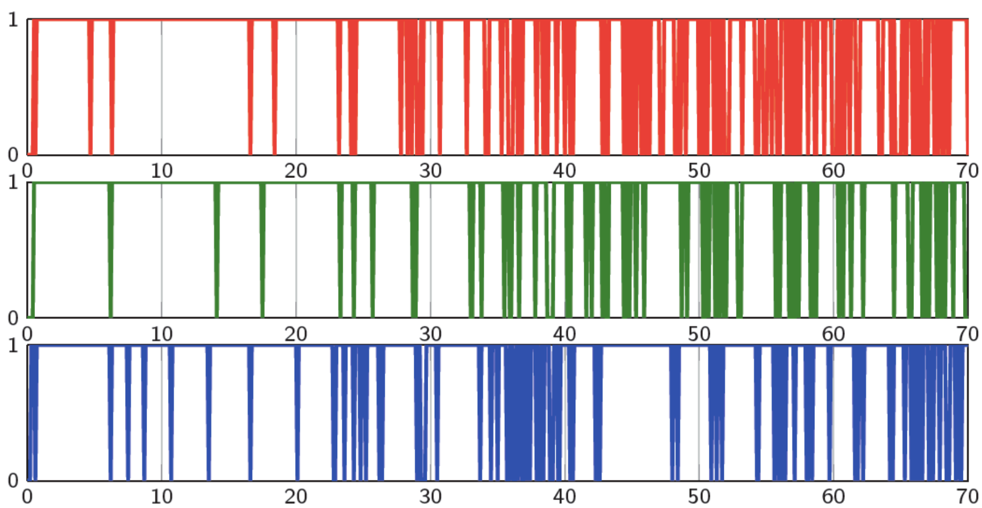

Fig. 11. Events